(1971); *ibid.*, **39**, 179 (1972).
(13) G. N. La Mar and F. A. Walker, *J. Am. Chem. Soc.*, **94**, 8607 (1972).
(14) E. V. Goldammer and H. Zorn, *Z. Naturforsch. B*, **31**, 242 (1976).
(15) E. V. Goldammer and H. Zorn, *Biophys. Chem.*, **3**, 249 (1975).
(16) J. D. Satterlee, G. N. La Mar, and J. S. Frye, *J. Am. Chem. Soc.*, **98**, 7275 (1976).
(17) J. W. Emsley, J. Feeney, and L. H. Sutcliffe, "High Resolution Nuclear Magnetic Resonance Spectroscopy", Vol. 1, Pergamon Press, London, 1965, Chapter 9; G. Binsch In "Dynamic Nuclear Magnetic Resonance Spectroscopy", L. M. Jackman and F. A. Cotton, Ed., Academic Press, New York, N.Y., 1975, Chapter 3.
(18) F. A. Walker, M.-W. Lo, and M. T. Ree, *J. Am. Chem. Soc.*, **98**, 5552 (1976).
(19) J. M. Duclos, *Bioinorg. Chem.*, **2**, 263 (1973); C. L. Coyle, P. A. Rafson, and E. H. Abbott, *Inorg. Chem.*, **12**, 2007 (1973).
(20) G. N. La Mar and F. A. Walker, *J. Am. Chem. Soc.*, **95**, 1782 (1973).
(21) J. D. Satterlee and G. N. La Mar, *J. Am. Chem. Soc.*, **98**, 2804 (1976).
(22) A. D. Adler, F. R. Longo, J. F. Finarreli, J. Goldmacher, J. Assour, and L. Korsakoff, *J. Org. Chem.*, **32**, 476 (1967).
(23) H. W. Whitlock and R. Hanauer, *J. Org. Chem.*, **33**, 2109 (1968).
(24) A. D. Adler, private communication.
(25) T. C. Farrar and E. D. Becker, "Pulse and Fourier Transform NMR", Academic Press, New York, N.Y., 1971, Chapter 2.
(26) G. N. La Mar and E. O. Sherman, *J. Am. Chem. Soc.*, **92**, 2691 (1970).
(27) Thus for [TPFFeCl] = 0.030 M, [1-CH_3Im] = 0.250 M, line width data yield $\tau_M^{-1} = 63 \pm 5\ s^{-1}$, and $\tau_f^{-1} = 22 \pm 4\ s^{-1}$. Since all of the complex is low-spin $P_M = 0.060$ M and $P_f = 0.190$ M, so that eq 5 is satisfied within experimental error.
(28) J. Hine, "Physical Organic Chemistry", McGraw-Hill, New York, N.Y., 1962, Chapter 4.
(29) Rate data for pyridine exchange for ferric complexes of natural porphyrin have been reported (ref 15), but these complexes exhibit a spin equilibrium. The indirect analysis of the kinetic process led the authors to conclude that in their case exchange occurred by an associative mechanism. The source of this discrepancy is not understood at this time.
(30) L. M. Epstein, D. K. Straub, and C. Maricondi, *Inorg. Chem.*, **6**, 1720 (1967).
(31) M. Momenteau, J. Mispelter, and D. Lexa, *Biochim. Biophys. Acta*, **320**, 652 (1973).
(32) J. S. Leigh, Jr., *J. Magn. Reson.*, **4**, 308 (1971).
(33) H. A. O. Hill and K. G. Morallee, *J. Am. Chem. Soc.*, **94**, 731 (1972).
(34) G. M. La Mar, G. R. Eaton, R. H. Holm, and F. A. Walker, *J. Am. Chem. Soc.*, **95**, 63 (1973); G. N. La Mar and F. A. Walker, *ibid.*, **95**, 6950 (1973).
(35) The fact that no shift is observed would require that the five-coordinate, high-spin complexes have a similar pyrrole-H shift as the low-spin complex, which is not considered likely (ref 13).

Stereochemistry of Manganese Porphyrins. 2. The Toluene Solvate of $\alpha,\beta,\gamma,\delta$-Tetraphenylporphinatomanganese(II) at 20 and −175 °C[1]

John F. Kirner,[2a,c] Christopher A. Reed,[2b] and W. Robert Scheidt* [2a]

Contribution from the Departments of Chemistry, University of Notre Dame, Notre Dame, Indiana 46556, and University of Southern California, Los Angeles, California 90007. *Received July 16, 1976*

Abstract: The crystal and molecular structure of the toluene solvate of $\alpha,\beta,\gamma,\delta$-tetraphenylporphinatomanganese(II) has been determined at 20 and −175 °C. This compound has been shown to bind oxygen reversibly at low temperatures. The compound crystallizes in the triclinic system, space group $P\bar{1}$. The unit cell has $a = 11.320$ (6), $b = 11.465$ (6), and $c = 10.487$ (6) Å, cos $\alpha = -0.3527$ (4), cos $\beta = -0.2307$ (4), and cos $\gamma = -0.3057$ (4), and $Z = 1$ at 20 °C and $a = 11.257$ (3), $b = 11.324$ (4), and $c = 10.367$ (4) Å, cos $\alpha = -0.3430$ (4), cos $\beta = -0.2227$ (3), and cos $\gamma = -0.3183$ (3), and $Z = 1$ at −175 °C. Measurement of diffracted intensities employed θ-2θ scans with graphite-monochromated Mo Kα radiation on a Syntex $P\bar{1}$ diffractometer. All independent reflections for $(\sin\theta)/\lambda \leq 0.742$ Å^{-1} (5640 unique observed data) were measured at 20 °C and for $(\sin\theta)/\lambda \leq 0.817$ Å^{-1} (6677 unique observed data) at −175 °C. These data were employed for the determination of structure using the heavy-atom method and full-matrix least-squares refinement. The final conventional and weighted discrepancy factors were 0.092 and 0.068 at 20 °C and 0.077 and 0.093 at −175 °C. The molecule has required C_i-$\bar{1}$ symmetry. The average Mn-N bond distance is in the range 2.082-2.092 Å, depending on the assumptions made in interpreting the least-squares refinements. The differences in the stereochemistry of the molecule at the two temperatures are minimal. The possible interaction of the toluene solvate molecules with the MnTPP molecule is discussed.

The determination of structure for high-spin four-coordinate $\alpha,\beta,\gamma,\delta$-tetraphenylporphinatomanganese(II),[3a] to be written as MnTPP, was undertaken with several considerations in view.

A most obvious consideration was to extend our structural knowledge for divalent metalloporphyrins of the first row transition elements. Previous study has established structure for all members of the *meso*-tetraphenylporphyrin series from iron(II) to copper(II).[4-7] The structure of MnTPP thus allowed further study of the structural changes concomitant with the stepwise addition or subtraction of a d electron. It should be pointed out that such an analysis, in principle rather straightforward, is complicated by the appearance of low-, intermediate-, and high-spin spectroscopic states as the metal ion, and hence the d electron configuration, is changed.

A second consideration deals with an interesting problem of macrocyclic structure, namely, the structural accommodation to a "mismatch" in the size of the central metal ion and the central hole of the macrocycle. Two "mismatch" cases are apparent. If the metal ion is too small for the size of the central hole, complex formation must lead to metal-ligand bonds that are stretched. If the metal ion is too large, positioning of the metal ion in the center of the macrocyclic hole must lead to compressed metal-ligand bond lengths relative to the normal values for complexes with monodentate ligands. In the latter case, which is the one of immediate interest, it is clear that there must be some limit to bond compression. However, several alternatives to excessive bond compression are possible. For porphyrins or other planar, quasi-rigid macrocycles a limited radial expansion of the central hole can occur.[8] More flexible macrocyclic ligands coordinate to an overlarge metal ion with ligand folding and thereby achieve normal metal-ligand bond distances.[9] Another alternative is to change the effective size of the metal ion. For some transition metal ions, this is accomplished by changing the spin state of the ion.[10] Thus for several square-planar iron(II) complexes,[4,11-13]

coordination of the iron(II) atom in an intermediate-spin ($S = 1$) rather than a high-spin state ($S = 2$) leads to a substantially smaller metal ion in the basal plane. The same situation pertains to intermediate-spin manganese(II) phthalocyanine.[11] Cobalt(II) macrocyclic complexes are generally low-spin rather than high-spin derivatives; a concomitant shortening of the basal ligand distances is observed. The macrocyclic ligand must have a reasonably strong ligand field to favor such spin pairing.

The most common structural adjustment to a size mismatch is a displacement of the metal atom out of the plane defined by the donor atoms of the macrocycle. However, centering of the metal atom in the ligand plane (in the four-coordinate case) must certainly lead to the strongest interaction between metal and ligand. When the metal atom is displaced, it is coordinated to a single axial ligand as well as to the donors of the macrocycle and is displaced toward the axial ligand. Examples of the resulting square-pyramidal complexes are adequately represented by the high-spin iron(II) and -(III) porphyrin derivatives[14] and five-coordinate zinc porphyrin[15] and phthalocyanine[16] complexes. Another appropriate example is provided by high-spin five-coordinate (1-methylimidazole)-α,β,γ,δ-tetraphenylporphinatomanganese(II),[3] whose structure was, however, unknown at the time this investigation was started. Out-of-plane displacements are also found for four-coordinate tin(II)[17] and lead(II)[18] phthalocyanines; in these two cases, the size mismatch is extreme.

The magnitude of the size mismatch between the high-spin spherically symmetric d^5 manganese(II) atom and the porphinato ligand would appear to be greater than that in the five-coordinate iron(II) and -(III) porphyrin derivatives, but less than that in the tin(II) and lead(II) phthalocyanine complexes; from these comparisons a substantial displacement of the manganese(II) atom could be anticipated.

Four-coordinate MnTPP crystallizes as the toluene solvate with a center of symmetry required for the molecule. Conventional least-squares refinement of room temperature diffraction data, with the manganese(II) atom positoned at the inversion center, leads to an unrealistically large thermal parameter for the metal atom (root-mean-square amplitude of 0.35 Å for vibration of the metal atom perpendicular to the mean plane of the porphinato core) and presents a problem of interpretation. This large thermal parameter suggests disorder in the position of the manganese(II) atom. A disorder model in which the metal atom is distributed between two symmetry-equivalent out-of-plane positions yields equally good agreement with the diffraction data. Such disorder of the manganese(II) atom could arise from either a static or dynamic process. Structure determination at low temperature promised to increase the theoretical resolution of the data and to decrease the thermal motion substantially. Either of these effects might aid in better understanding the system. Consequently, structural data for MnTPP were also collected at low temperature (−175 °C) and the results of both structure determinations are presented herein. Our results for MnTPP also prompted the study of a related system, zinc phthalocyanine, in which the size mismatch was expected to be comparable in magnitude to MnTPP; the results of that investigation are presented in the following paper.[19]

We[3a] and others[3b] have communicated that MnTPP is the precursor of a reversible oxygen adduct. Full synthetic details and further characterization will be forthcoming.

Experimental Section

Crystals of the toluene solvate of MnTPP were mounted in thin-walled capillaries in a nitrogen-filled drybox. Preliminary x-ray photographic examination established a one-molecule triclinic unit cell. The choice of centrosymmetric $P\bar{1}$ as the space group was confirmed by the successful refinement and through an analysis of the E statistics.[20] Least-squares refinement of the setting angles of 22 reflections, each collected at $\pm 2\theta$, led to the cell constants listed in Table I. For a cell content of $MnN_4C_{44}H_{28}\cdot 2C_7H_8$, the calculated density is 1.261 g/cm³. An accurate experimental density was not obtained owing to the extreme air sensitivity of the compound.

Table I. Summary of Crystal Data and Intensity Collection

Temp	20 °C	−175 °C
a, Å	11.320 (6)	11.257 (3)
b, Å	11.465 (6)	11.324 (4)
c, Å	10.487 (6)	10.367 (4)
Cos α	−0.3527 (4)	−0.3430 (4)
Cos β	−0.2307 (4)	−0.2227 (3)
Cos γ	−0.3057 (4)	−0.3183 (3)
Volume, Å³	1121.9	1092.1
Calcd density, g/cm³	1.261	1.295
Z	1	1
Radiation	Graphite-monochromated Mo Kα (λ 0.71069 Å)	
μ, mm^{-1}	0.329	0.338
Scan range	0.7° below $K\alpha_1$ to 0.7° above $K\alpha_2$	0.8° below $K\alpha_1$ to 0.8° above $K\alpha_2$
Background	0.5 times scan time at extremes of scan	Profile analysis
2θ limits	3.5–63.7°	3.5–71.0°
Criterion for observation	$F_o > 2\sigma(F_o)$	$F_o > 3\sigma(F_o)$
Unique obsd data	5640	6677

Intensity data were measured on a Syntex $P\bar{1}$ four-circle diffractometer using graphite-monochromated Mo Kα radiation and θ–2θ scanning. Variable 2θ scan rates were used according to the intensity of the reflection and ranged from 2.0 to 6.0°/min. Background counts were collected at the extremes of the scan for 0.5 times the time required for the scan itself. Two crystals, with approximate dimensions of 0.21 × 0.24 × 0.27 and 0.17 × 0.25 × 0.42 mm, were employed for data collection. Four standard reflections, measured every 50 reflections during data collection, showed a small monotonic decrease in intensity (2 and 8%) and a linear correction was applied to the data. Trial absorption corrections showed that the neglect of absorption effects would cause errors of less than 2% in the value of structure amplitudes and no correction was therefore applied. Intensity data were reduced and standard deviations calculated as described previously.[21] A total of 5640 unique reflections having $(\sin\theta)/\lambda \leq 0.742$ Å^{-1} and $F_o > 2\sigma(F_o)$ were considered observed (73% of the theoretical number possible) and were used in the solution and refinement of structure.

The structure was solved by the heavy-atom method[22a] and refined by full-matrix least-squares techniques.[22b] In the later stages of refinement, two blocks were used because of computer storage limitations. A difference Fourier synthesis, calculated after isotropic refinement, revealed electron density concentrations appropriately located for the porphyrin hydrogen atoms; these positions and the positions of the toluene ring hydrogen atoms were idealized (C–H = 0.95 Å, $B(H) = B(C) + 1.0$ Å²) and included in the refinement as fixed contributors. Anisotropic refinement of all heavy atoms was carried to convergence with the manganese(II) atom positioned at the center of symmetry. The final values of the discrepancy indices were $R_1 = \sum||F_o| - |F_c||/\sum|F_o| = 0.092$ and $R_2 = [\sum w(|F_o| - |F_c|)^2/\sum w(F_o)^2]^{1/2} = 0.068$. The estimated standard deviation of an observation of unit weight was 1.345. The largest shift/error was 0.10; the largest peak in the final difference Fourier map was 0.55 e/Å³ and was in the region of the manganese atom.

The large value of the thermal parameter of the manganese atom for vibration perpendicular to the mean plane of the core (rms amplitude = 0.35 Å, $B = 9.7$ Å²) suggested positional disorder of the manganese(II) atom. A disorder model in which the metal atom was distributed between two symmetry-equivalent out-of-plane positions was then attempted. This refinement converged at the same R values

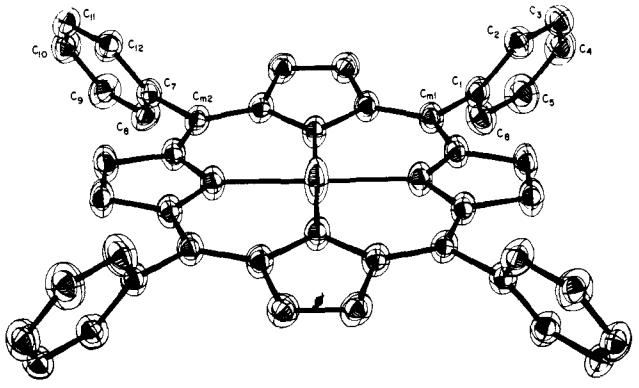

Figure 1. Computer-drawn model in perspective of the MnTPP molecule. Atoms are represented by their vibrational ellipsoids contoured to enclose 50% of the electron density. Inner ellipsoids represent atoms at −175 °C, the outer ellipsoids represent the atoms at 20 °C.

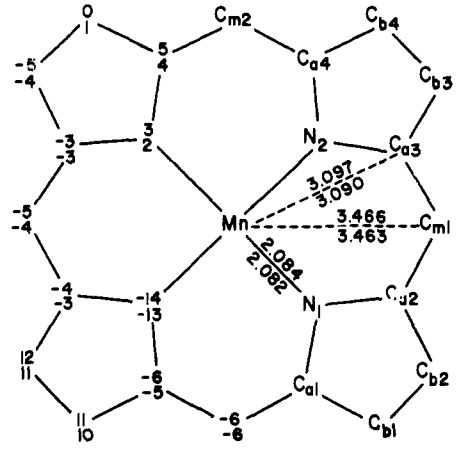

Figure 2. Formal diagram of the porphinato core illustrating the numbering scheme and the displacement of the atoms from the mean plane of the core. The right hand side of the diagram gives the labels assigned to each unique atom. On the left hand side of the centrosymmetric diagram, the label identifying each atom has been replaced by the displacement of the atom from the mean plane of the core, in units of 0.01 Å. The upper value of each pair of values is the value observed at −175 °C, the lower value is that observed at 20 °C. Also displayed are some important radii of the core at the two temperatures.

Table II. Atomic Coordinates in the Unit Cell (−175 °C)[a]

Atom[b] type	Coordinates × 10^4		
	x	y	z
Mn	0	0	0
N(1)	1486 (2)	370 (2)	1892 (2)
N(2)	55 (2)	1951 (2)	1100 (2)
$C_a(1)$	2084 (2)	−489 (2)	2021 (2)
$C_a(2)$	2092 (2)	1554 (2)	3219 (2)
$C_a(3)$	772 (2)	2841 (2)	2583 (2)
$C_a(4)$	−820 (2)	2440 (2)	570 (2)
$C_b(1)$	3108 (2)	178 (2)	3495 (2)
$C_b(2)$	3118 (2)	1442 (2)	4227 (2)
$C_b(3)$	344 (2)	3941 (2)	3008 (2)
$C_b(4)$	−648 (2)	3692 (2)	1772 (2)
$C_m(1)$	1760 (2)	2701 (2)	3550 (2)
$C_m(2)$	−1775 (2)	1797 (2)	−882 (2)
C(1)	2522 (2)	3873 (2)	5073 (2)
C(2)	2349 (2)	3699 (2)	6307 (2)
C(3)	3052 (2)	4797 (3)	7723 (2)
C(4)	3942 (2)	6085 (3)	7933 (2)
C(5)	4133 (3)	6267 (3)	6717 (3)
C(6)	3425 (3)	5168 (2)	5298 (2)
C(7)	−2569 (2)	2558 (2)	−1247 (2)
C(8)	−1928 (2)	3827 (2)	−1265 (2)
C(9)	−2647 (2)	4557 (2)	−1572 (3)
C(10)	−4033 (2)	4025 (3)	−1874 (3)
C(11)	−4692 (2)	2747 (3)	−1882 (2)
C(12)	−3963 (2)	2026 (2)	−1562 (2)
C(13)	8013 (3)	745 (3)	3168 (3)
C(14)	7144 (3)	546 (3)	1839 (4)
C(15)	6865 (3)	−537 (3)	509 (3)
C(16)	7449 (3)	−1450 (3)	461 (4)
C(17)	8324 (3)	−1256 (4)	1767 (4)
C(18)	8601 (3)	−177 (4)	3097 (4)
C(19)	8325 (5)	1940 (4)	4618 (4)

[a] The number in parentheses following each datum is the estimated standard deviation in the least significant figure. [b] Atoms are identified in agreement with Figures 1 and 2.

as the refinement above. The largest shift/error and the largest peak in a final difference Fourier synthesis were also quite similar. Thus from crystallographic criteria, neither model can be regarded as superior. The temperature factor for the manganese atom was still quite large (rms amplitude 0.28 Å). It should also be noted that the final displacement of the manganese(II) atom of ±0.19 Å out-of-plane leads to a Mn···Mn separation that is slightly smaller than the minimum resolution of the data (0.411 Å).[23]

Intensity data were also collected at −175.5 ± 1.5 °C[24] employing a Syntex LT-1 low-temperature attachment for the automated diffractometer. Crystal data at this temperature are listed in Table I. During the course of measurements, it became necessary to warm the crystal back to room temperature twice; no deleterious effects were noted. Intensity data were processed in the same manner as before, with the exception that background counts were estimated from an analysis of peak profiles,[25] A total of 6677 unique reflections having $(\sin\theta)/\lambda \leq 0.817$ Å^{-1} and $F_o > 3\sigma(F_o)$ were considered observed (67% of the number possible) and were used in the subsequent refinements.

Full-matrix least-squares refinement was commenced using final positional parameters from the 20 °C refinement and isotropic temperature factors. A difference Fourier synthesis showed electron density concentrations appropriately located for the hydrogen atoms; these positions were idealized as before and included in the refinement as fixed contributors. Anisotropic refinement of all heavy atoms was carried to convergence with the manganese(II) atom positioned at the center of symmetry. The last stages of refinement again utilized two blocks. The final value of R_1 was 0.077; R_2 was 0.093. The largest shift/errors were less than 10%. The final difference Fourier had no significant features; the largest peak was 0.8 e/Å^3 (5–7% of the height of a typical carbon atom) and was in the vicinity of the manganese atom. The estimated standard deviation of an observation of unit weight was 1.95.

The thermal parameter of the manganese(II) atom for vibration perpendicular to the mean plane of the core was again large (rms amplitude = 0.24 Å). The disorder model in which the metal atom was distributed between two symmetry-equivalent out-of-plane positions was attempted. This refinement, with an initial out-of-plane displacement of the manganese(II) atom of ±0.25 Å and an isotropic temperature factor, converged; the manganese(II) atom was displaced by ±0.177 Å. Further refinement, with the position of the manganese held constant and refined anisotropic temperature factors, converged at $R_1 = 0.079$ and $R_2 = 0.095$. Attempts to simultaneously refine the anisotropic temperature factors and position of the manganese(II) atom failed; the position of the metal atom gradually drifted toward the center of symmetry. The refinement was terminated when the Mn···Mn separation had decreased to well below the minimum resolution of the data (0.373 Å). It should be noted that this refinement utilized 1101 data of higher resolution than that of the 20 °C refinement.

Atomic coordinates derived from the −175 °C refinement are listed in Table II and those from the 20 °C refinement are listed in Table III.[26] The associated thermal parameters from both refinements are listed in Table IV. Listings of the observed and calculated structure factors for both data sets are available.[26] Bond lengths and angles are listed in Tables V–IX. The numbering scheme employed for the several atoms is that displayed in Figures 1 and 2. Primed and unprimed

Table IV. Thermal Parameters[a]

Atom type	Anisotropic parameters						
	B_{11}	B_{22}	B_{33}	B_{12}	B_{13}	B_{23}	B,[b] Å^2
Mn	2.68 (2)	1.62 (2)	1.23 (2)	1.18 (2)	−0.60 (1)	0.02 (1)	1.70
	5.45 (3)	3.19 (2)	2.99 (2)	2.54 (2)	−1.23 (2)	0.07 (1)	3.55
N(1)	1.54 (6)	1.48 (6)	1.19 (5)	0.59 (5)	0.32 (4)	0.48 (4)	1.48
	3.32 (7)	2.86 (6)	2.40 (6)	1.43 (5)	0.11 (5)	0.83 (5)	2.96
N(2)	1.36 (5)	1.52 (6)	1.14 (5)	0.56 (5)	0.17 (4)	0.51 (4)	1.40
	2.96 (6)	2.79 (6)	2.53 (6)	1.33 (5)	0.18 (5)	0.85 (5)	2.87
C_a(1)	1.41 (7)	1.63 (7)	1.23 (6)	0.58 (5)	0.29 (5)	0.65 (5)	1.45
	2.95 (7)	3.19 (7)	2.65 (7)	1.45 (6)	0.33 (5)	1.26 (6)	2.93
C_a(2)	1.52 (7)	1.57 (7)	1.10 (6)	0.57 (5)	0.31 (5)	0.54 (5)	1.44
	3.28 (8)	3.06 (7)	2.26 (7)	1.35 (6)	0.24 (5)	0.88 (5)	2.99
C_a(3)	1.30 (6)	1.44 (7)	1.17 (6)	0.46 (5)	0.24 (5)	0.47 (5)	1.40
	3.04 (7)	2.5 (7)	2.49 (7)	1.28 (6)	0.37 (5)	0.83 (5)	2.91
C_a(4)	1.35 (6)	1.46 (7)	1.28 (6)	0.57 (5)	0.38 (5)	0.61 (5)	1.39
	2.74 (7)	2.70 (6)	2.88 (7)	1.14 (6)	0.46 (5)	1.06 (5)	2.90
C_b(1)	1.79 (7)	1.98 (8)	1.24 (6)	0.90 (6)	0.21 (5)	0.64 (5)	1.65
	4.10 (9)	4.02 (9)	2.72 (8)	2.10 (8)	0.05 (6)	1.18 (6)	3.54
C_b(2)	1.77 (7)	2.05 (8)	1.16 (6)	0.86 (6)	0.13 (5)	0.51 (5)	1.69
	3.99 (9)	4.12 (9)	2.48 (8)	2.02 (8)	−0.17 (6)	0.87 (6)	3.53
C_b(3)	1.62 (7)	1.51 (7)	1.29 (6)	0.66 (5)	0.46 (5)	0.40 (5)	1.54
	3.43 (8)	3.07 (8)	2.90 (8)	1.47 (7)	0.70 (6)	0.75 (6)	3.32
C_b(4)	1.60 (7)	1.56 (7)	1.46 (6)	0.70 (6)	0.50 (5)	0.58 (5)	1.58
	3.33 (8)	3.00 (7)	3.34 (8)	1.69 (6)	0.84 (6)	1.03 (6)	3.25
C_m(1)	1.49 (7)	1.53 (7)	1.04 (6)	0.59 (5)	0.26 (5)	0.44 (5)	1.42
	3.07 (8)	2.91 (7)	2.34 (7)	1.20 (6)	0.33 (5)	0.79 (5)	2.96
C_m(2)	1.20 (6)	1.59 (7)	1.29 (6)	0.51 (5)	0.31 (5)	0.71 (5)	1.37
	2.68 (7)	2.95 (7)	2.97 (8)	1.19 (6)	0.57 (5)	1.43 (6)	2.89
C(1)	1.48 (7)	1.59 (7)	1.06 (6)	0.63 (5)	0.26 (5)	0.33 (5)	1.46
	3.28 (8)	3.34 (8)	2.33 (7)	1.63 (6)	0.28 (6)	0.72 (6)	3.08
C(2)	1.81 (8)	2.08 (8)	1.26 (6)	0.71 (6)	0.50 (5)	0.65 (6)	1.74
	4.10 (10)	4.56 (10)	2.95 (9)	1.93 (8)	0.99 (7)	1.27 (7)	3.95
C(3)	2.03 (8)	2.82 (10)	1.05 (6)	1.24 (7)	0.49 (6)	0.59 (6)	1.82
	4.79 (11)	6.63 (14)	2.63 (8)	3.25 (11)	1.21 (7)	1.40 (8)	4.26
C(4)	1.96 (8)	2.24 (9)	1.24 (6)	0.91 (7)	0.24 (6)	0.03 (6)	1.91
	4.80 (11)	4.75 (11)	3.18 (10)	2.30 (10)	0.32 (8)	0.02 (8)	4.48
C(5)	2.13 (9)	1.78 (8)	1.71 (7)	0.23 (7)	0.19 (6)	0.25 (6)	2.16
	5.29 (13)	3.84 (10)	3.97 (11)	0.96 (9)	0.43 (9)	0.42 (8)	4.97
C(6)	2.20 (8)	1.85 (8)	1.32 (6)	0.50 (6)	0.36 (6)	0.48 (6)	1.94
	4.71 (11)	3.78 (9)	3.06 (9)	1.17 (8)	0.54 (7)	0.93 (7)	4.22
C(7)	1.38 (6)	1.70 (7)	1.18 (6)	0.69 (5)	0.32 (5)	0.65 (5)	1.41
	3.12 (8)	3.08 (7)	2.80 (7)	1.57 (6)	0.70 (6)	1.27 (6)	2.98
C(8)	1.43 (7)	1.91 (8)	1.80 (7)	0.71 (6)	0.50 (5)	1.01 (6)	1.65
	3.18 (8)	3.82 (9)	4.45 (10)	1.62 (7)	1.06 (7)	2.18 (8)	3.67
C(9)	2.12 (8)	2.11 (8)	2.00 (8)	1.10 (7)	0.73 (6)	1.25 (6)	1.87
	4.89 (11)	4.21 (10)	5.36 (12)	2.54 (9)	1.78 (9)	2.95 (9)	4.23
C(10)	2.08 (8)	2.83 (10)	1.75 (7)	1.58 (7)	0.81 (6)	1.24 (7)	1.87
	4.95 (11)	5.56 (12)	4.34 (11)	3.57 (10)	1.53 (8)	2.75 (9)	4.14
C(11)	1.45 (7)	2.77 (9)	1.62 (7)	1.08 (6)	0.49 (5)	1.07 (6)	1.76
	3.29 (9)	6.04 (12)	3.98 (10)	2.69 (9)	1.17 (7)	2.42 (9)	3.95
C(12)	1.43 (7)	2.05 (8)	1.63 (7)	0.70 (6)	0.48 (5)	0.91 (6)	1.68
	3.03 (8)	4.22 (9)	3.81 (9)	1.55 (7)	0.96 (7)	2.05 (7)	3.62
C(13)	2.5 (1)	2.9 (1)	2.5 (1)	0.3 (1)	1.1 (1)	1.2 (1)	2.7
	6.4 (2)	6.4 (2)	7.9 (2)	1.1 (1)	3.1 (2)	3.3 (2)	6.9
C(14)	2.2 (1)	2.6 (1)	3.6 (1)	0.8 (1)	1.4 (1)	1.7 (1)	2.6
	5.5 (2)	6.8 (2)	9.1 (2)	1.9 (1)	3.0 (2)	4.7 (2)	6.6
C(15)	2.2 (1)	3.2 (1)	2.7 (1)	0.5 (1)	0.8 (1)	1.7 (1)	2.6
	6.3 (2)	6.9 (2)	7.5 (2)	1.3 (1)	2.4 (2)	3.5 (2)	7.1
C(16)	2.8 (1)	2.6 (1)	3.2 (1)	0.6 (1)	1.6 (1)	1.3 (1)	2.8
	6.5 (2)	6.9 (2)	8.3 (2)	1.3 (2)	4.0 (2)	3.6 (2)	6.9
C(17)	2.4 (1)	3.3 (1)	4.6 (2)	1.3 (1)	1.6 (1)	2.4 (1)	3.0
	6.8 (2)	7.7 (2)	13.9 (4)	3.3 (2)	5.5 (2)	6.7 (3)	7.7
C(18)	2.3 (1)	3.9 (1)	3.4 (1)	0.7 (1)	0.4 (1)	2.3 (1)	3.0
	6.1 (2)	8.5 (2)	8.5 (2)	1.5 (2)	1.2 (2)	5.0 (2)	7.6
C(19)	5.4 (2)	3.7 (2)	3.2 (1)	0.4 (1)	2.2 (1)	0.7 (1)	4.2
	16.0 (5)	8.0 (3)	10.3 (4)	2.7 (3)	6.7 (3)	1.5 (2)	11.3

[a] For each atom, the first line gives thermal parameters from data collected at −175 °C; the second line, from data collected at 20 °C. The number following each datum is the estimated standard deviation in the least significant figure. B_{ij} is related to the dimensionless β_{ij} employed during refinement as $B_{ij} = 4\beta_{ij}/a_i^* a_j^*$. [b] Isotropic thermal parameters as calculated from $B = 4[V^2 \det(\beta_{ij})]^{1/3}$.

Table V. Bond Lengths in the Coordination Group and Porphinato Skeleton (−175 °C)[a]

Type	Length, Å	Type	Length, Å	Type	Length, Å
Mn-N(1)	2.085 (2)	$C_a(1)$-$C_b(1)$	1.450 (3)	$C_a(4)$-$C_b(4)$	1.451 (3)
Mn-N(2)	2.082 (2)	$C_a(1)$-$C_m(2)'$	1.414 (3)	$C_a(4)$-$C_m(2)$	1.408 (3)
N(1)-$C_a(1)$	1.373 (3)	$C_a(2)$-$C_b(2)$	1.445 (3)	$C_b(1)$-$C_b(2)$	1.366 (3)
N(1)-$C_a(2)$	1.375 (2)	$C_a(2)$-$C_m(1)$	1.416 (3)	$C_b(3)$-$C_b(4)$	1.366 (3)
N(2)-$C_a(3)$	1.376 (2)	$C_a(3)$-$C_b(3)$	1.450 (3)	$C_m(1)$-C(1)	1.492 (3)
N(2)-$C_a(4)$	1.378 (2)	$C_a(3)$-$C_m(1)$	1.411 (3)	$C_m(2)$-C(7)	1.498 (3)

[a] The numbers in parentheses are the estimated standard deviations.

Table VI. Bond Lengths in the Coordination Group and Porphinato Skeleton (20 °C)[a]

Type	Length, Å	Type	Length, Å	Type	Length, Å
Mn-N(1)	2.084 (2)	$C_a(1)$-$C_b(1)$	1.448 (2)	$C_a(4)$-$C_b(4)$	1.443 (3)
Mn-N(2)	2.079 (2)	$C_a(1)$-$C_m(2)'$	1.414 (3)	$C_a(4)$-$C_m(2)$	1.413 (2)
N(1)-$C_a(1)$	1.368 (2)	$C_a(2)$-$C_b(2)$	1.445 (2)	$C_b(1)$-$C_b(2)$	1.351 (3)
N(1)-$C_a(2)$	1.368 (2)	$C_a(2)$-$C_m(1)$	1.410 (3)	$C_b(3)$-$C_b(4)$	1.358 (3)
N(2)-$C_a(3)$	1.370 (2)	$C_a(3)$-$C_b(3)$	1.445 (3)	$C_m(1)$-C(1)	1.494 (2)
N(2)-$C_a(4)$	1.370 (2)	$C_a(3)$-$C_m(1)$	1.413 (2)	$C_m(2)$-C(7)	1.495 (2)

[a] The numbers in parentheses are the estimated standard deviations.

Table VII. Bond Angles in the Coordination Group and Porphinato Skeleton (−175 °C)[a]

Angle	Value, deg	Angle	Value, deg
N(1)MnN(2)	90.27 (7)	$C_a(1)C_b(1)C_b(2)$	107.1 (2)
$C_a(1)N(1)C_a(2)$	107.4 (2)	$C_a(2)C_b(2)C_b(1)$	107.1 (2)
$C_a(3)N(2)C_a(4)$	107.6 (2)	$C_a(3)C_b(3)C_b(4)$	107.1 (2)
$N(1)C_a(1)C_m(2)'$	125.3 (2)	$C_a(4)C_b(4)C_b(3)$	107.3 (2)
$N(1)C_a(1)C_b(1)$	109.1 (2)	$C_a(2)C_m(1)C_a(3)$	126.4 (2)
$C_m(2)'C_a(1)C_b(1)$	125.6 (2)	$C_a(2)C_m(1)C(1)$	116.9 (2)
$N(1)C_a(2)C_m(1)$	125.4 (2)	$C_a(3)C_m(1)C(1)$	116.7 (2)
$N(1)C_a(2)C_b(2)$	109.3 (2)	$C_a(4)C_m(2)C_a(1)'$	126.5 (2)
$C_m(1)C_a(2)C_b(2)$	125.3 (2)	$C_a(4)C_m(2)C(7)$	116.8 (2)
$N(2)C_a(3)C_m(1)$	125.8 (2)	$C_a(1)'C_m(2)C(7)$	116.7 (2)
$N(2)C_a(3)C_b(3)$	109.1 (2)	$MnN(1)C_a(1)$	126.5 (1)
$C_m(1)C_a(3)C_b(3)$	125.0 (2)	$MnN(1)C_a(2)$	126.1 (1)
$N(2)C_a(4)C_m(2)$	125.7 (2)	$MnN(2)C_a(3)$	125.3 (1)
$N(2)C_a(4)C_b(4)$	109.0 (2)	$MnN(2)C_a(4)$	125.8 (1)
$C_m(2)C_a(4)C_b(4)$	125.2 (2)		

[a] The numbers in parentheses are the estimated standard deviations.

Table VIII. Bond Angles in the Coordination Group and Porphinato Skeleton (20 °C)[a]

Angle	Value, deg	Angle	Value, deg
N(1)MnN(2)	90.16 (6)	$C_a(1)C_b(1)C_b(2)$	107.1 (2)
$C_a(1)N(1)C_a(2)$	107.7 (1)	$C_a(2)C_b(2)C_b(1)$	107.3 (2)
$C_a(3)N(2)C_a(4)$	107.7 (1)	$C_a(3)C_b(3)C_b(4)$	107.0 (2)
$N(1)C_a(1)C_m(2)'$	125.5 (2)	$C_a(4)C_b(4)C_b(3)$	107.4 (2)
$N(1)C_a(1)C_b(1)$	108.9 (2)	$C_a(2)C_m(1)C_a(3)$	126.1 (2)
$C_m(2)'C_a(1)C_b(1)$	125.6 (2)	$C_a(2)C_m(1)C(1)$	117.1 (2)
$N(1)C_a(2)C_m(1)$	125.8 (2)	$C_a(3)C_m(1)C(1)$	116.8 (2)
$N(1)C_a(2)C_b(2)$	108.9 (2)	$C_a(4)C_m(2)C_a(1)'$	126.0 (2)
$C_m(1)C_a(2)C_b(2)$	125.2 (2)	$C_a(4)C_m(2)C(7)$	116.9 (2)
$N(2)C_a(3)C_m(1)$	125.9 (2)	$C_a(1)'C_m(2)C(7)$	117.1 (2)
$N(2)C_a(3)C_b(3)$	109.1 (1)	$MnN(1)C_a(1)$	126.4 (1)
$C_m(1)C_a(3)C_b(3)$	125.0 (2)	$MnN(1)C_a(2)$	125.9 (1)
$N(2)C_a(4)C_m(2)$	126.0 (2)	$MnN(2)C_a(3)$	125.5 (1)
$N(2)C_a(4)C_b(4)$	108.9 (2)	$MnN(2)C_a(4)$	125.7 (1)
$C_m(2)C_a(4)C_b(4)$	125.1 (2)		

[a] The numbers in parentheses are the estimated standard deviations.

symbols, e.g., C_i and C_i', denote a pair of atoms related by the center of symmetry wherein the manganese(II) atom is positioned.

Discussion

Figure 1 is a computer-drawn model[27] in perspective of the MnTPP molecule as it exists in the crystal. The figure also illustrates the difference in the thermal vibrations of the atoms at the two different temperatures used for data collection. The inner ellipsoids, scaled at the 50% probability level, are those appropriate for the molecule at the low temperature. The outer, simpler ellipsoids, on the same probability scale as the first set, have a size concomitant with the thermal parameters for the molecule at 20 °C (Table IV). Both sets of ellipsoids are centered at the atomic positions listed in Table II.

For the porphinato core, the dimensional variations in bond lengths and angles of chemically analogous bond types differ immaterially from fourfold geometry. In addition, the effect of temperature on the observed bond lengths and angles is small. Using C_a and C_b to denote the respective α- and β-carbon atoms of a pyrrole ring, and C_m for methine carbon, the averaged bond lengths and angles of a given chemical type in the porphine skeleton are listed in Table X. The first set of average values listed are those observed at −175 °C; the second set are those at 20 °C. The first number in parentheses following each averaged length is the mean deviation from the average value in units of 0.001 Å and the second is the value of the estimated standard deviation for an individually determined length.[28] It is seen that the differences in values of a given chemical type for the two MnTPP data sets are minimal except perhaps for the C_b-C_b lengths. The low-temperature value for C_b-C_b appears to be the more probable when the variation of porphinato core parameters with radial expansion of the core is considered, cf. Table X. It may be further noted that the C_b-C_b bonds are the most likely set of bonds in the porphinato core to be foreshortened by thermal motion.

However, the apparent bond distances of the peripheral phenyl groups and the toluene solvate are substantially affected by the temperature. Individually determined bond distances

Table IX. Bond Lengths in the Phenyl Groups and Toluene Molecule[a]

Type	Length, Å	Type	Length, Å	Type	Length, Å
C(1)-C(2)	1.405 (3)	C(7)-C(8)	1.397 (3)	C(13)-C(14)	1.397 (4)
	1.386 (3)		1.388 (3)		1.376 (5)
C(2)-C(3)	1.390 (3)	C(8)-C(9)	1.391 (3)	C(14)-C(15)	1.380 (4)
	1.397 (3)		1.385 (3)		1.335 (5)
C(3)-C(4)	1.390 (4)	C(9)-C(10)	1.396 (4)	C(15)-C(16)	1.384 (5)
	1.370 (4)		1.379 (4)		1.339 (6)
C(4)-C(5)	1.396 (4)	C(10)-C(11)	1.396 (4)	C(16)-C(17)	1.383 (5)
	1.370 (4)		1.373 (4)		1.379 (6)
C(5)-C(6)	1.393 (3)	C(11)-C(12)	1.394 (3)	C(17)-C(18)	1.379 (5)
	1.393 (3)		1.390 (3)		1.414 (6)
C(6)-C(1)	1.396 (3)	C(12)-C(7)	1.402 (3)	C(18)-C(13)	1.393 (5)
	1.383 (3)		1.392 (3)		1.377 (6)
				C(13)-C(19)	1.510 (5)
					1.533 (6)

[a] For each bond length, the first line is the result calculated from data collected at −175 °C; the second line, from data collected at 20 °C. The numbers in parentheses are the estimated standard deviations.

Table X. Averaged Bond Lengths and Angles of the Chemical Classes in the Porphinato Cores of Selected Metalloporphyrins[a]

Porphyrin	Length, Å, of				
	Ct···N	$N-C_a$	C_a-C_m	C_a-C_b	C_b-C_b
MnTPP (−175 °C)	2.084 (2)	1.376 (2,2)	1.412 (2,3)	1.449 (2,3)	1.366 (0,3)
MnTPP (20 °C)	2.082 (2)	1.369 (1,2)	1.412 (2,3)	1.445 (1,3)	1.354 (3,3)
Cl_2SnTPP[b]	2.098 (2)	1.370 (2)	1.407 (2)	1.446 (3)	1.380 (3)
Pip_2FeTPP[c]	2.004 (2)	1.384 (2)	1.396 (3)	1.444 (5)	1.347 (4)
Pip_2CoTPP[d]	1.987 (2)	1.380 (2)	1.392 (2)	1.444 (3)	1.344 (3)
NiOEP[e]	1.929 (4)	1.387 (3)	1.373 (4)	1.448 (5)	1.362 (5)

Porphyrin	Value, deg, of					
	C_aNC_a	NC_aC_b	NC_aC_m	$C_aC_bC_b$	$C_aC_mC_a$	$C_mC_aC_b$
MnTPP (−175 °C)	107.5 (1,2)	109.1 (1,2)	125.5 (2,2)	107.1 (1,2)	126.4 (1,2)	125.3 (2,2)
MnTPP (20 °C)	107.6 (1,1)	108.9 (0,2)	125.8 (2,2)	107.2 (1,2)	126.0 (1,2)	125.2 (2,2)
Cl_2SnTPP[b]	109.2 (2)	108.2 (2)	126.4 (2)	107.2 (1)	126.4 (2)	125.4 (2)
Pip_2FeTPP[c]	105.2 (3)	110.2 (3)	125.6 (3)	107.2 (3)	124.1 3(	124.1 (3)
Pip_2CoTPP[d]	104.8 (1)	110.5 (2)	125.8 (2)	107.0 (2)	123.4 (2)	123.6 (2)
NiOEP[e]	105.1	110.7	124.0	106.8	124.1	125.0

[a] The first number in parentheses following each averaged length or angle for MnTPP is the mean deviation in units of 0.001 Å or 0.1°, the second is the value of the estimated standard deviation of an individually determined length. For all other derivatives the number in parentheses is the estimated standard deviation.[28] [b] Dichloro-α,β,γ,δ-tetraphenylporphinatotin(IV), ref 8. [c] Bis(piperidine)-α,β,γ,δ-tetraphenylporphinatoiron(II), ref 29. [d] Bis(piperidine)-α,β,γ,δ-tetraphenylporphinatocobalt(II), ref 21. [e] Octaethylporphinatonickel(II), ref 30.

are listed in Table IX. The average C-C bond distance for the phenyl groups at 20 °C is 1.384 (7,4) Å; the average at −175 °C is 1.396 (3,4) Å. The average C-C distance at −175 °C is seen to be almost exactly the standard value for the aromatic C-C separation. Furthermore, the mean deviation from the average is halved at the low temperature. These observations are consistent with a dampening of the complex thermal motions of the phenyl groups, which lead to foreshortened C-C bond distances at the higher temperature. This matter has been discussed previously.[8] Even more striking differences occur for the toluene molecule: the average ring C-C distance at 20 °C is 1.370 (20,6) Å; at −175 °C, the C-C distance is 1.386 (6,5) Å. The effect of temperature on the value of the C-C-C angles is minimal; in all cases the average internal angle is 120.0°.

Figure 2, a formal diagram of the porphinato core, displays the perpendicular displacement, in units of 0.01 Å, of each unique atom from the mean plane of the core. The upper value of each pair of values is the displacement observed for the molecule at −175 °C; the lower value is the observed value at 20 °C. The centrosymmetrically related atoms in the right hand portion of the diagram have displacements of the same magnitude, but opposite sign. It is seen (Figure 2) that the temperature has little effect on the conformation of the porphinato core and, further, that the departures from planarity are unremarkable for porphyrin derivatives. Local flatness is maintained and individual pyrrole rings are planar to within 0.005 Å. The angle between the normals to the mean plane of the core and to the pyrrole ring containing N(1) is 2.5°; the corresponding angle with the N(2) pyrrole ring is 6.6° (at −175 °C). The dihedral angles between the plane of the core and the planes of the phenyl groups are 70.4 and 67.0° at 20 °C and 68.0 and 66.1° at −175 °C. The smaller dihedral angles at −175 °C reflect the slightly larger packing density at the lower temperature.

Also entered in Figure 2 are some important radii of the core. All radii are seen to be slightly, although not significantly, larger at low temperature. The average distance from Ct, the center of the molecule, to the porphyrin nitrogen atoms is 2.084 (2,2) (−175 °C) or 2.082 (2,2) Å (20 °C). The average value of Ct···N corresponds to the minimum value of the Mn-N bond distance. An out-of-plane displacement of the manganese atom

Table XI. Complexing Bond Lengths in a Sequence of Four-Coordinate Metallotetraphenylporphyrins and Metallophthalocyanines

Metal ion	d^5 Mn	d^6 Fe	d^7 Co	d^8 Ni	d^9 Cu
		Tetraphenylporphinato			
M-N distance, Å	2.082-2.092	1.972 (4)	1.949 (3)	1.928 (3)	1.981 (7)
Spin state, S	5/2	1	1/2	0	1/2
Ref	*a*	*b*	*c*	*d*	*e*
		Phthalocyanato			
M-N distance, Å	1.938 (3)	1.926 (1)		~1.83	1.934 (6)
Spin state, S	3/2	1	1/2	0	1/2
Ref	*f*	*f*		*g*	*h*

[a] This work. [b] Reference 4. [c] Reference 5. [d] Reference 6. [e] Reference 7. [f] Reference 11. [g] Reference 36. [h] Reference 37.

will increase the Mn-N bond distance. The calculated displacement of the manganese atom from the least-squares refinement (cf. Experimental Section) probably reflects maximum values for an out-of-plane displacement; using these manganese atom positions leads to calculated Mn-N bond distances of 2.092 (−175 °C) and 2.091 Å (20 °C), which are the probable maximum Mn-N bond distances. The observed thermal motion of the manganese atom is distinctly different from that observed for several four-coordinate metalloporphyrins[4-7] and metallophthalocyanines,[11,37] including ZnPc,[19] and provides strong evidence against an equilibrium centering of the manganese atom in the porphinato core. In other words, the positioning of the manganese atom at the center of the core corresponds to a subsidiary maximum in the potential energy. For a sufficiently large potential barrier, the manganese atoms in the centrosymmetric crystal would be equally distributed between two sets of equilibrium positions. With a low barrier, cooperative thermal motion of the metal atom and atoms of the core would allow the metal atom to pass freely between the two equilibrium positions of minimum potential energy. Either case is consistent with the observed structural data.

The probable range of Mn-N bond distances, 2.082-2.092 Å, in high-spin MnTPP is shorter, but comparable to, the 2.128-Å average Mn-N_p bond distance in high-spin five-coordinate (1-methylimidazole)-*meso*-tetraphenylporphinatomanganese(II).[3,31] The Mn^{II}-N distances are significantly larger than the 2.01-2.03-Å range observed for several high-spin, five- or six-coordinate manganese(III) porphyrins[1,32-34] and the 2.028-Å average Mn-N_p distance found in low-spin six-coordinate nitrosyl(4-methylpiperidine)-*meso*-tetraphenylporphinatomanganese(II).[35] The relatively long bonds in the high-spin manganese(II) porphyrins are correlated with the (singly) occupied $d_{x^2-y^2}$ orbital; this orbital is unoccupied in the high-spin manganese(III) and low-spin manganese(II) derivatives, which have relatively short Mn-N bond distances. This correlation is also seen in the complexing M-N bond lengths in the sequence of four-coordinate metalloporphyrins and metallophthalocyanines displayed in Table XI. Particularly noteworthy is the short Mn-N bond distance in intermediate-spin MnPc; the $d_{x^2-y^2}$ orbital is unoccupied in this derivative.

The average Mn-N bond distance in MnTPP is somewhat longer than the average Fe-N_p bond distance of 2.065 Å in the isoelectronic high-spin iron(III) porphyrins.[14] The iron(III) porphyrins, which are all five-coordinate derivatives with an axial anionic ligand, have the iron(III) atom displaced by ~0.45 Å out of the mean porphinato plane and a Ct···N radius of ~2.015 Å. Thus the geometry of the MN_4 group is substantially more pyramidal in the iron(III) derivatives than in MnTPP, where the maximum displacement is ~0.19 Å and Ct···N is 2.084 Å. Given the generally accepted conclusion that the porphyrin core resists undue radial expansion in the mean plane,[8] it is pertinent to ask why the MnTPP molecule displays a substantially expanded core and a less pyramidal geometry

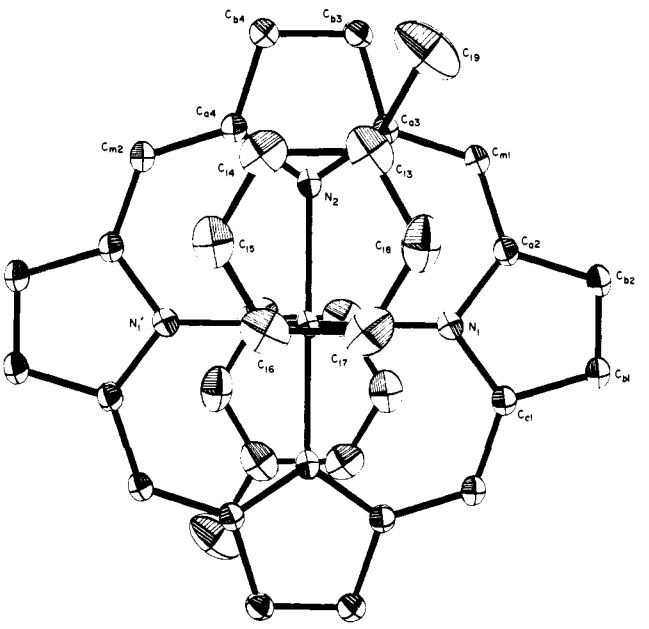

Figure 3. A view of the MnTPP molecule illustrating the relationship between the toluene molecules and the porphyrin. The porphinato plane lies parallel to the plane of the paper. Phenyl rings have been omitted. Vibrational ellipsoids are at the 50% probability level (−175 °C).

than the isoelectronic iron(III) derivatives. The larger out-of-plane displacement of the iron atom minimizes nonbonded contacts between the axial ligand and atoms of the core, a consideration which does not apply to the four-coordinate MnTPP molecule. The less pyramidal geometry of the MnTPP molecule also allows for greater overlap between the bonding orbitals on the metal and the porphyrin ligand. Further, the core appears to be expanded sufficiently that the thermally excited vibrations can allow the metal atom to pass freely through the porphyrin plane.[38] Finally, the interaction of the toluene molecules with the MnTPP molecule may stabilize a smaller out-of-plane displacement of the manganese(II) atom (vide infra).

Figures 3 and 4 display the centrosymmetric relationship between the two toluene molecules of crystallization and the MnTPP molecule. The dihedral angle between the toluene plane and the mean plane of the core is 10.7°. The N(2) pyrrole plane is tilted such that the dihedral angle between its plane and the toluene plane is reduced to 6.7°. The interplanar spacing between the toluene plane and the N(2) pyrrole ring is 3.52 Å.[39] The average perpendicular distance between the six atoms of the toluene ring and the mean plane of the core is 3.30 Å. The Mn···C(16) distance is 3.05 Å; Mn···C(17) is 3.25 Å.[40]

The geometry and interplanar distances[41-42] suggest the possibility of weak π-complex formation between the toluene

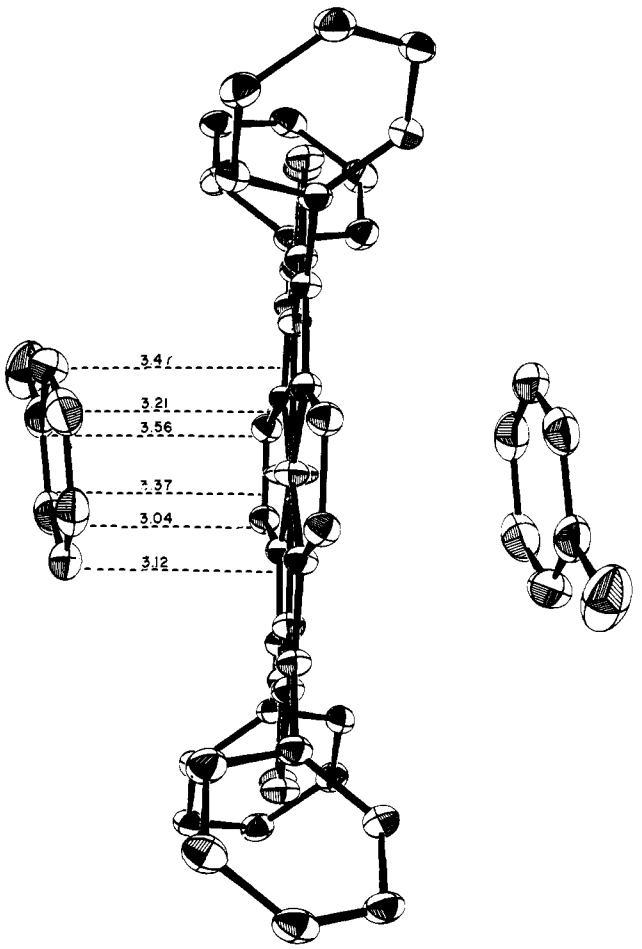

Figure 4. A second view of the MnTPP molecule illustrating the relationship between the toluene molecules and the porphyrin. The porphinato plane is approximately perpendicular to the plane of the paper. Perpendicular distances between toluene atoms and the mean porphinato plane are shown. Vibrational ellipsoids are at the 50% probability level (−175 °C). Note the large vibrational component of the manganese atom perpendicular to the mean plane.

and metalloporphyrin. π complexes of porphyrins and metalloporphyrins have been known for some time[43] and have been the subject of several recent investigations.[44-47] Hill et al.[44] have shown that the small donors dimethylaniline and hexamethylbenzene form weak complexes with manganese(III) porphyrins. Walker[46] suggested 2:1 complex formation with Co(p-OCH_3)TPP and toluene at low temperatures. La Mar[47] has suggested from NMR experiments, for cobalt(II) porphyrin complexes, that the π interaction occurs exclusively at the periphery of the porphyrin ring and does not involve the metal directly. It is clear, however, in the present case, that if a π interaction occurs between the toluene and MnTPP, that interaction must involve the metal directly. Such interactions in this 2:1 (centrosymmetric) complex should limit the displacement of the metal out-of-plane. Other than the close intermolecular contacts between toluene and MnTPP, there are no significantly short intermolecular contacts.

Acknowledgment. We are grateful for support for this research from the National Institutes of Health (HL-15627) and the Research Corporation.

Supplementary Material Available: Table III, atomic coordinates of MnTPP at 20 °C; Table XII, root-mean-square amplitudes of vibration; and listings of the structure factor amplitudes (62 pages). Ordering information is given on any current masthead page.

References and Notes

(1) Part 1: J. F. Kirner and W. R. Scheidt, *Inorg. Chem.*, **14**, 2081 (1975).
(2) (a) University of Notre Dame; (b) University of Southern California; (c) taken in part from a dissertation presented to the Graduate School in partial fulfillment of the requirements for the Ph.D., 1976.
(3) (a) A preliminary account of a portion of this work has appeared; B. Gonzalez, J. Kouba, S. Yee, C. A. Reed, J. F. Kirner, and W. R. Scheidt, *J. Am. Chem. Soc.*, **97**, 3247 (1975); (b) C. J. Weschler, B. M. Hoffman, and F. Basolo, *ibid.*, **97**, 5278 (1975).
(4) FeTPP: J. P. Collman, J. L. Hoard, N. Kim, G. Lang, and C. A. Reed, *J. Am. Chem. Soc.*, **97**, 2676 (1975).
(5) CoTPP: P. Madura and W. R. Scheidt, *Inorg. Chem.*, **15**, 3182 (1976).
(6) NiTPP: A. A. Saylor and J. L. Hoard, to be submitted for publication.
(7) CuTPP: E. B. Fleischer, C. K. Miller, and L. E. Webb, *J. Am. Chem. Soc.*, **86**, 2342 (1964).
(8) D. M. Collins, W. R. Scheidt, and J. L. Hoard, *J. Am. Chem. Soc.*, **94**, 6689 (1972).
(9) D. H. Busch, K. Farmery, V. Goedken, V. Katovic, A. C. Melnyk, C. R. Sperati, and N. Tokel, *Adv. Chem. Ser.*, **No. 100**, 44 (1971), and references cited therein.
(10) The stabilization of one oxidation state over another when coordinated to certain macrocycles might well be considered as another example of this alternative.
(11) J. F. Kirner, W. Dow, and W. R. Scheidt, *Inorg. Chem.*, **15**, 1685 (1976).
(12) R. G. Little, J. A. Ibers, and J. E. Baldwin, *J. Am. Chem. Soc.*, **97**, 7049 (1975).
(13) S. Koch, R. H. Holm, and R. B. Frankel, *J. Am. Chem. Soc.*, **97**, 6714 (1975).
(14) J. L. Hoard in "Porphyrins and Metalloporphyrins", K. M. Smith, Ed., Elsevier, Amsterdam, 1975, Chapter 8; W. R. Scheidt in "The Porphyrins", D. Dolphin, Ed., Academic Press, New York, N.Y., in press.
(15) D. M. Collins and J. L. Hoard, *J. Am. Chem. Soc.*, **92**, 3761 (1970); D. L. Cullen and E. F. Meyer, Jr., American Crystallographic Association, Summer Meeting, Aug 1971, Abstract No. K15.
(16) T. Kobayashi, T. Ashida, N. Uyeda, E. Suito, and M. Kakudo, *Bull. Chem. Soc. Jpn.*, **44**, 2095 (1971).
(17) M. K. Friedel, B. F. Hoskins, R. L. Martin, and S. A. Mason, *Chem. Commun.*, 400 (1970).
(18) K. Ukei, *Acta Crystallogr., Sect. B.*, **29**, 2290 (1973).
(19) W. R. Scheidt and W. Dow, *J. Am. Chem. Soc.*, following paper in this issue.
(20) I. L. Karle, K. S. Dragonette, and S. A. Brenner, *Acta Crystallogr.*, **19**, 713 (1965).
(21) W. R. Scheidt, *J. Am. Chem. Soc.*, **96**, 84 (1974).
(22) (a) A locally modified version of the Fourier program ALFF, written in PL/1, was used: C. R. Hubbard, C. o. Quicksall, and R. A. Jacobson, Ames Laboratory, Iowa State University, Ames, Iowa, 1971, Report No. IS-2625. (b) A local modification of ORFLS was employed. W. R. Busing, K. O. Martin, and H. A. Levy, "OR-FLS, A Fortran Crystallographic Least-Squares Program", Oak Ridge National Laboratory, Oak Ridge, Tenn., 1962, Report No. ORNL-TM-305. Atomic form factors were from D. T. Cromer and J. B. Mann, *Acta Crystallogr., Sect. A.*, **24**, 321 (1968), with real and imaginary corrections for anomalous dispersion in the form factor of the manganese atom from D. T. Cromer and D. Liberman, *J. Chem. Phys.*, **53**, 1891 (1970). Scattering factors for hydrogen from R. F. Stewart, F. R. Davidson, and W. T. Simpson, *J. Chem. Phys.*, **42**, 3175 (1965).
(23) R. W. James, "The Optical Principles of the Diffraction of Xrays", G. Bell and Sons, London, England, 1965, p 400.
(24) The temperature of the cold stream was measured using a calibrated iron–constantan thermocouple in a configuration similar to that described by R. D. Burbank (*J. Appl. Crystallogr.*, **6**, 437 (1973)). The stationary thermocouple was coaxial to the nitrogen cold stream with the probe at the center of the four-circle goniometer. The temperature varied by only 3 °C during a 2-h period. Data collection was simulated by slewing the diffractomer axis; no effect on the temperature could be detected. However, during actual data collection, the temperature of the crystal is expected to vary more than is indicated by the static experiments owing to turbulence of the nitrogen stream caused by the glass capillary, angle movements, and icing of the capillary. We estimate these temperature excursions to be no more than 20 °C.
(25) Calculations were performed using a local modification of a program described by R. Blessing, P. Coppens, and P. Becker, *J. Appl. Crystallogr.*, **7**, 488 (1974).
(26) Supplementary material.
(27) C. K. Johnson, "ORTEP, a Fortran Thermal-Ellipsoid Plot Program for Crystal Structure Illustrations", Oak Ridge National Laboratory, Oak Ridge, Tenn., 1965, Report No. ORNL-3794.
(28) This notation for reporting averaged values of both bond lengths and angles is used throughout the discussion.
(29) L. J. Radonovich, A. Bloom, and J. L. Hoard, *J. Am. Chem. Soc.*, **94**, 2073 (1972).
(30) E. F. Meyer, Jr., *Acta Crystallogr., Sect. B*, **28**, 2162 (1972).
(31) J. F. Kirner, C. A. Reed, and W. R. Scheidt, *J. Am. Chem. Soc.*, in press.
(32) L. J. Radonovich and J. L. Hoard, personal communication.
(33) B. M. L. Chen and A. Tulinsky, personal communication.
(34) V. W. Day, B. R. Stults, E. L. Tasset, R. O. Day, and R. S. Marianelli, *J. Am. Chem. Soc.*, **96**, 2650 (1974); V. W. Day, B. R. Stults, E. L. Tasset, R. S. Marianelli, and L. J. Boucher, *Inorg. Nucl. Chem. Lett.*, 11, 505 (1975).
(35) P. L. Piciulo, G. Rupprecht, and W. R. Scheidt, *J. Am. Chem. Soc.*, **96**, 5293 (1974).
(36) J. M. Robertson and I. Woodward, *J. Chem. Soc.*, 219 (1937).
(37) C. J. Brown, *J. Chem. Soc. A*, 2488 (1968).
(38) A symmetric motion of the four nitrogen atoms of 0.05–0.07 Å away from Ct would increase Ct···N to 2.13–2.15 Å. Such motion appears quantitatively

possible even at −175 °C. Confer Table XII, which gives the root-mean-square amplitudes of vibration of all atoms at both temperatures.
(39) This value is the average perpendicular distance between N(2) and the toluene plane and C(13) and C(14) and the N(2) pyrrole plane.
(40) All distances are those observed at −175 °C.
(41) The 3.52-Å separation between the organic portions is at the upper limit of values observed for π complexes; the 3.30-Å separation between the toluene molecule and the porphyrin core is a typical separation: F. H. Herbstein, "Perspectives in Structural Chemistry", Vol. IV, J. D. Dunitz and J. A. Ibers, Ed., Wiley, New York, N.Y., 1971, Chapter 3.
(42) The larger spacing at the toluene methyl portion of the ring may well result from steric interactions between the methyl group and atoms of the porphyrin. See Figure 4. Spacings (3.5 Å) are observed for hexamethylbenzene complexes.[41]
(43) A. Treibs, *Justus Liebigs Ann. Chem.*, **476**, 1 (1929).
(44) H. A. O. Hill, A. J. MacFarlane, and R. J. P. Williams, *J. Chem. Soc. A*, 1704 (1969).
(45) H. A. O. Hill, P. J. Sadler, R. J. P. Williams, and C. D. Barry, *Ann. N.Y. Acad. Sci.*, **206**, 247 (1973).
(46) F. A. Walker, *J. Magn. Reson.*, **15**, 201 (1974).
(47) G. P. Fulton and G. N. LaMar, *J. Am. Chem. Soc.*, **98**, 2119 (1976); G. P. Fulton and G. N. LaMar, *ibid.*, 2124 (1976).

Molecular Stereochemistry of Phthalocyanatozinc(II)

W. Robert Scheidt* and W. Dow

Contribution from the Department of Chemistry, University of Notre Dame, Notre Dame, Indiana 46556. *Received July 16, 1976*

Abstract: The molecular stereochemistry of phthalocyanatozinc(II) (ZnPc) has been determined by x-ray diffraction methods. The phthalocyanato ligand constrains the zinc atom to effectively square-planar coordination. Surprisingly, the zinc atom has contracted sufficiently to fit into the central hole of the phthalocyanato ligand; the zinc atom is centered or very nearly centered in the plane of the four phthalocyanato nitrogen atoms. The core of the phthalocyanato ligand is somewhat expanded with the average Zn-N bond distance = 1.980 (2) Å. A comparison of the stereochemical parameters of the expanded core of ZnPc with those of the relatively contracted core of FePc shows that the alterations accompanying expansion of the phthalocyanato core are similar to those noted previously for porphyrin derivatives. Crystal data: space group, $P2_1/a$; a = 19.274 (5), b = 4.8538 (15), c = 14.553 (4) Å, β = 120.48 (2)°; ρ_{exptl} = 1.62 and ρ_{calcd} = 1.614 g/cm^3 for Z = 2; required molecular symmetry, $\bar{1}$. Intensity data were measured by θ-2θ scanning on a Syntex P$\bar{1}$ automated diffractometer using graphite-monochromated Mo Kα radiation. The intensities of 4515 unique observed data with $(\sin\theta)/\lambda \leq 0.935$ Å^{-1} were used in the refinement of the 187 structural parameters. Final discrepancy indices: R_1 = 0.060; R_2 = 0.073.

The genesis of our interest in the molecular structure of four-coordinate phthalocyanatozinc(II), ZnPc, has been outlined in the preceding paper.[1] Appraisal of known zinc-nitrogen bond distances in various coordination geometries suggests that the zinc(II) atom is too large to fit into the central hole of the phthalocyanato ligand. Of particular interest is the structure of the five-coordinate *n*-hexylamine adduct of phthalocyanatozinc(II).[2] The zinc(II) atom is displaced 0.48 Å from the basal plane of the phthalocyanato nitrogen atoms; the average phthalocyanato nitrogen-zinc bond distance is 2.06 Å. The Zn-N bond distances in five-coordinate porphyrin derivatives are slightly larger at 2.07 Å; the displacement of the zinc atom slightly smaller at 0.31-0.33 Å.[3,4] Hence ZnPc could be expected to provide an analogous example to the structure observed for *meso*-tetraphenylporphinatomanganese(II).[1] Our earlier studies of MnPc and FePc,[5] in addition to providing useful standards of reference for an analysis of thermal vibrations in the crystal, indicated that crystals of ZnPc could be expected to yield a data set containing a large number of high-resolution reflections. This expectation was met, and we report herein the molecular stereochemistry of ZnPc derived from measurements corresponding to a theoretical resolution[6] of 0.326 Å (2θ = 83.3) with Mo Kα radiation.

Experimental Section

ZnPc was prepared by a published procedure[7] and purified by vacuum sublimation. Single crystals, suitable for x-ray study, were grown by vacuum sublimation in quartz tubes at ~450 °C under a nitrogen atmosphere. Crystals used in the analysis were cut from larger needles. All measurements were derived from a specimen measuring 0.15 × 0.15 × 0.66 mm.

Preliminary photographic examination showed that ZnPc crystallized as the well-known β-polymorph. The space group $P2_1/a$ [C_{2h}^5, No. 14],[8] a nonstandard choice, was chosen to conform to earlier choices of unit cells for phthalocyanato derivatives.[9] Lattice constants, a = 19.274 (5), b = 4.8538 (15), c = 14.553 (4) Å, and β = 120.48 (2)° (λ 0.71069 Å), came from a least-squares refinement that utilized the setting angles of 30 reflections, each collected at $\pm 2\theta$, given by the automatic centering routine supplied with the Syntex P$\bar{1}$ diffractometer. All measurements were made at the ambient laboratory temperature of 20 ± 1 °C. The calculated density for two molecules per unit cell was 1.614 g/cm^3; the measured density was 1.62 g/cm^3.

X-ray intensity data were collected using graphite-monochromated Mo Kα radiation on a computer-controlled four-circle diffractometer, using θ-2θ scanning to a 2θ limit of 83.3° ($(\sin\theta)/\lambda$ = 0.935 Å^{-1}). The scan range was 1.1° on either side of the Kα_1, Kα_2 doublet. Scan rates varied from 1.0 to 8.0°, with most reflections being measured at the slowest scan rate. Background counts were estimated from an analysis of the reflection profiles using a local modification of a program recently described.[10] Four standard reflections, measured every 50 reflections during data collection, displayed no trend with exposure to the x-ray beam. With the cited dimensions of the crystal and a linear absorption coefficient of 1.10 mm^{-1}, the error in intensity from neglect of absorption effects was seen to be less than 3%; this was confirmed by ψ scans and no correction was applied. Intensity data were reduced and standard deviations calculated as described previously.[11] Data were retained as objectively observed if $F_o > 3\sigma(F_o)$, leading to 4515 unique observed data (56% of the theoretical number possible).

Atomic coordinates reported for CuPc[12] were used for the initial coordinates in the asymmetric unit of structure (one-half of the ZnPc molecule). Full-matrix least-squares refinement[13] converged smoothly using isotropic temperature factors for all atoms and standard values[14,15] for atomic form factors. Difference Fourier syntheses[16] gave electron density concentrations appropriately located for all hydrogen atom positions; these positions were idealized (C-H = 0.95 Å) with temperature factors fixed one unit higher than that of the associated carbon atom. Subsequent refinement used anisotropic temperature factors for all heavy atoms and fixed hydrogen contributors and was carried to convergence. The final parameter shifts were less than 10% of the estimated standard deviations during the last cycle. Final values of the discrepancy indices $R_1 = \Sigma[|F_o| -$